

A 3D Beamforming Analytical Model for 5G Wireless Networks

Jean-Marc Kelif¹, Marceau Coupechoux², Mathieu Mansanarez³

Abstract—This paper proposes an analytical study of 3D beamforming for 5G wireless networks. In a first step, we develop a three dimensional analytical beamforming model for wireless networks. This 3D model enables in particular, to focus the analyzes on the specific zone covered by an antenna beam. This 3D beamforming model is validated by comparison with Monte Carlo simulations: the two approaches give very close SINR (Signal to Interference plus Noise Ratio) values. Thanks to this model, it becomes easy to quantify the impact of 3D beamforming in terms of performance, quality of service and coverage in a future 5G wireless network. Different scenarios are presented, which quantify the impact of the 3D beamforming wireless network and show the accuracy of the model. The proposed model is then used to compare 2D and 3D beamforming and to show the interest of exploiting the third dimension.

I. INTRODUCTION

There are many candidate features to improve peak and average data rates in future cellular networks (see for example [1]) and that need to be evaluated. 3D beamforming is one of them and is the subject of this paper.

A. Beamforming Techniques

To date, horizontal beamforming techniques are already implemented. This improvement has already been proven and allows to enhance the signal strength at the UE's location. A recent research goes further and shows us the possibility of combining the vertical dimension with the horizontal dimension. Adaptation of the vertical beam pattern in addition to the horizontally applied multi-antenna scheme is the key element for the extension towards 3D beamforming. This technique offers a better spectral efficiency and a better control of cell edge throughput. Different realization options for vertical downtilt adaptation have been considered so far in the literature: (a) One fixed downtilt applied in the entire cell. This is the baseline case; (b) A main lobe steering directly to the terminal with possibly additional limitation of the lowest possible downtilt; (c) The selection of one out of several fixed downtilts, depending on the location of the terminal.

¹Jean-Marc Kelif is with Orange Labs, France. Email: jean-marc.kelif@orange.com

²Marceau Coupechoux is with LTCI, Telecom ParisTech, France. Email: marceau.coupechoux@telecom-paristech.fr

J.-M. Kelif and M. Coupechoux are partly supported by the french ANR project NETLEARN ANR-13-INFR-004.

³Mathieu Mansanarez is with Telecom ParisTech, France. Email: mathieu.mansanarez@gmail.com

B. Related Works

Reference [2] studies cell splitting based on active antennas. Authors study the expected gain brought by two fixed downtilts and a scheme with six beams per site. In the former scenario, the cell is split into two parts: a near and a far area. Each area is associated to a fixed downtilt. Performance evaluation is carried out using system level simulations in a urban environment. The results exhibit an increase in throughput of 27% for the horizontal beamforming with six beams per site and up to 62% for the vertical beamforming with two fixed downtilts over the base-line trisectorized case.

Reference [3] shows the potential of 3D beamforming and provides some performance results obtained from lab and field trial setups. In this requirement, the dynamic adaptation of the transmitted signal by the eNode-B is realized by means of a feedback sent by the UEs. The trials are performed in indoor and outdoor deployments in Line-Of-Sight (LOS) and No-Line-Of-Sight (NLOS) conditions. The results state that, regardless of the propagation conditions (LOS or NLOS), the adaptive 3D beamforming offers system performance improvements by using the reflections of the signals. Authors stress that two signals can be sent on the same radio resource for two different UEs and still can be separated at the receivers. The paper concludes that 3D beamforming can significantly improve the system performance but without giving numerical results or implicit comparison with classical beamforming.

The cornerstone of [4] is to reduce the effect of inter-cell interference by using Fractional Frequency Reuse (FFR) Technique. A cell is classically divided in three sectors. As for other FFR techniques, a sector is divided into a cell-center and a cell-edge area, to which different sub-carriers are allocated. Contrary to classical schemes, each area is associated to a unique downtilt. Authors use system level simulations to study the performance of their technique. Simulation results show that the SINR can be greatly improved at cell edge using the proposed scheme.

Reference [5] focuses on the interference avoidance by using dynamic vertical beamsteering for a limited macro-cell. For this purpose, this paper distinguishes two types of coordination methods: with and without the requirement of control information exchange between eNodes-B. Without information exchange, the best cell edge throughputs are obtained by using three fixed downtilts. In terms of maximum spectral efficiency, the dynamic scheme with limited downtilt is the best solution. When information exchange is locally allowed, dynamic beam steering with lower bound on the tilt provides better performance with 30% gain in cell edge user throughput

for a same spectral efficiency than one fixed downtilt and 10% gain in spectral efficiency for a same cell edge user throughput. Two fixed downtilts give intermediates results. Some field trials in real deployments are also introduced. Authors consider a single-cell scenario without any interference and analyze the behavior of 3D antenna pattern on the terminal for typical environmental conditions.

Reference [6] investigates the capability to use the vertical dimension in order to compensate the higher carrier which will be employed for future cellular networks. Indeed, this technique allows to decrease the path-loss without boosting the transmit power or scaling down the cell size. Simulation results show that this system allows to maintain the overall spectral efficiency in the entire cell in spite of the higher carrier.

Reference [7] examines the impact of 3x2 vertical sectorization (3 sectors, 2 downtilts) by comparing different parameters like various vertical half-power bandwidths and downtilt angles (implemented with a Remote Electrical Tilt). It also evaluates the performance of MIMO Spatial Multiplexing (SM) & Space Time Transmit Diversity (STTD) in comparison with 1x2 Maximal Ratio Combining (MRC) and SISO antenna systems. For 3GPP case 3 model, the cell throughput with the 3x2 vertical sectorization is 10 times higher than a 3 sectors setup for SISO systems. Similar comparisons are obtained for MIMO and SIMO schemes.

We see from this review that the performance of 3D beamforming depends on many parameters such as the number of available tilts, their combination, whether tilts are fixed or not, and other parameters not mentioned above like 3 dB horizontal and vertical beamwidths. To the best of our knowledge, the literature on system level performance evaluation of 3D beamforming relies either on simulations or field trials. A need thus arises for an analytical model able to provide very quick results in many different scenarios.

Our Contribution: In this paper, we develop a three dimensional beamforming analytical model for wireless networks. We establish a closed form formula of the Signal to Interference plus Noise Ratio (SINR), validated by comparisons with Monte Carlo simulations. We show that this formula is particularly well-suited to analyze beamforming impacts. This formula enables to analyze different scenarios of 3D beamforming deployments in terms of performance and quality of service, in an easy way.

The paper is organized as follows. In Section II, we develop the 3D beamforming analytical network model. We moreover establish the analytical expression of the SINR by using this model. In Section III, the validation of this analytical 3D model is done by comparison with Monte Carlo simulations. Section IV conducts a beamforming analysis using the proposed model and compares 2D and 3D beamforming. Section V concludes the paper.

II. SYSTEM MODEL

We consider a wireless network consisting of S geographical sites, each one composed by 3 base stations. Each antenna covers a sectored cell. We focus our analysis on the downlink, in the context of an OFDMA based wireless network, with frequency reuse 1. Let us consider:

- $\mathcal{S} = \{1, \dots, S\}$ the set of geographic sites, uniformly and regularly distributed over a two-dimensional plane.
- $\mathcal{N} = \{1, \dots, N\}$ the set of base stations, uniformly and regularly distributed over the two-dimensional plane. The base stations are equipped with directional antennas: $N = 3S$.
- the antenna height, denoted h .
- F sub-carriers $f \in \mathcal{F} = \{1, \dots, F\}$ where we denote W the bandwidth of each sub-carrier.
- $P_f^{(j)}(u)$ the transmitted power assigned by the base station j to sub-carrier f towards user u .
- $g_f^{(j)}(u)$ the propagation gain between transmitter j and user u in sub-carrier f .

We assume that time is divided into slots. Each slot consists in a given sequence of OFDMA symbols. As usual at network level, we assume that there is no Inter-Carrier Interference (ICI) so that there is no intra-cell interference.

The total amount of power received by a UE u connected to the base station i , on sub-carrier f is given by the sum of: a useful signal $P_f^{(i)}(u)g_f^{(i)}(u)$, an interference power due to the other transmitters $\sum_{j \in \mathcal{N}, j \neq i} P_f^{(j)}(u)g_f^j(u)$ and thermal noise power N_{th} .

We consider the SINR $\gamma_f(u)$ defined by:

$$\gamma_f(u) = \frac{P_f^{(i)}(u)g_f^{(i)}(u)}{\sum_{j \in \mathcal{N}, j \neq i} P_f^{(j)}(u)g_f^j(u) + N_{th}} \quad (1)$$

as the criterion of radio quality.

We investigate the quality of service and performance issues of a network composed of sites equipped with 3D directional transmitting antennas. The analyzed scenarios consider that all the subcarriers are allocated to UEs (full load scenario). Consequently, each sub-carrier f of any base station is used and can interfere with the ones of other sites. All sub-carriers are independent, we can thus focus on a generic one and drop the index f .

A. Expression of the SINR

Let us consider the path-gain model $g(R) = KR^{-\eta}A$, where K is a constant, R is the distance between a transmitter t and a receiver u , and $\eta > 2$ is the path-loss exponent. The parameter A is the antenna gain (assuming that receivers have a 0 dBi antenna gain).

Therefore, for a user u located at distance R_i from its serving base station i , the expression (1) of the SINR can be expressed, for each sub-carrier (dropping the index f):

$$\gamma(R_i, \theta_i, \phi_i) = \frac{G_0PKR_i^{-\eta}A(\theta_i, \phi_i)}{G_0 \sum_{j \in \mathcal{N}, j \neq i} PKR_j^{-\eta}A(\theta_j, \phi_j) + N_{th}}, \quad (2)$$

where:

- P is the transmitted power,
- $A(\theta_i, \phi_i)$ is the pattern of the 3D transmitting antenna of the base station i , and G_0 is the maximum antenna gain.
- θ_j is the horizontal angle between the UE and the principal direction of the antenna j ,

- ϕ_j is the vertical angle between the UE and the antenna j (see Fig. 1),
- $R_i = \sqrt{r_i^2 + h^2}$, where r_i represents the projection of R_i on the ground.

The gain $G(\theta, \phi)$ of an antenna in a direction (θ, ϕ) is defined as the ratio between the power radiated in that direction and the power that radiates an isotropic antenna without losses. This property characterizes the ability of an antenna to focus the radiated power in one direction. The parameter G_0 (2) is particularly important for a beamforming impact analysis. Let notice that it is determined by considering that the power, which would be transmitted in all directions for a non directive antenna (with a solid angle of 4π), is transmitted in a solid angle given by the horizontal and the vertical apertures of the antenna. In the ideal case where the antenna emits in a cone defined by $0 \leq \theta \leq \theta_{3dB}$ and $0 \leq \phi \leq \phi_{3dB}$, the gain is given by $\frac{4\pi}{\int \int A(\theta, \phi) \sin\theta d\theta d\phi}$.

B. BS Antenna Pattern

In our analysis, we conform to the model of [8] for the antenna pattern (gain, side-lobe level). The antenna pattern which is applied to our scheme, is computed as:

$$A_{dB}(\theta, \phi) = -\min[-(A_{h_{dB}}(\theta) + A_{v_{dB}}(\phi)), A_m], \quad (3)$$

where $A_h(\theta)$ and $A_v(\phi)$ correspond respectively to the horizontal and the vertical antenna patterns.

The horizontal antenna pattern used for each base station is given by:

$$A_{h_{dB}}(\theta) = -\min\left[12\left(\frac{\theta}{\theta_{3dB}}\right)^2, A_m\right], \quad (4)$$

where:

- θ_{3dB} is the half-power beamwidth (3 dB beamwidth);
- A_m is the maximum attenuation.

The vertical antenna direction is given by:

$$A_{v_{dB}}(\phi) = -\min\left[12\left(\frac{\phi - \phi_{tilt}}{\phi_{3dB}}\right)^2, A_m\right], \quad (5)$$

where:

- ϕ_{tilt} is the downtilt angle;
- ϕ_{3dB} is the 3 dB beamwidth.

1) *Antenna Pattern in the Network*: Each site is constituted by 3 antennas (3 sectors). Therefore, for any site s of the network, we have :

$$\begin{cases} A_h(\theta_s^2) = A_h(\theta_s^1 + 2\frac{\pi}{3}) \\ A_h(\theta_s^3) = A_h(\theta_s^1 - 2\frac{\pi}{3}) \\ A_v(\phi_s^1) = A_v(\phi_s^2) = A_v(\phi_s^3), \end{cases} \quad (6)$$

where θ_s^a and ϕ_s^a represent the angles relative to the antenna $a \in \{1, 2, 3\}$ for the site s . For the sake of simplicity, in expression (2) we do a sum on the base stations (not on the sites) and denote θ_j and ϕ_j the angles relative to the antenna j .

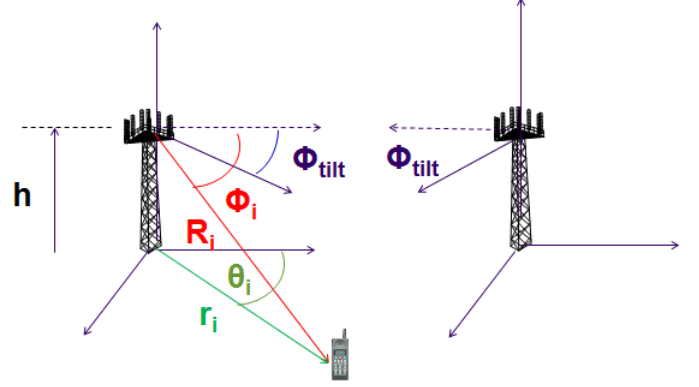


Figure 1. User equipment located at (r_i, θ_i) . It receives a useful power from antenna i and interference power from antenna j .

2) *Vertical Antenna Gain in the Network*: For a UE at the distance r_j from the antenna j , the vertical angle can be expressed as:

$$\phi_j = \arctan\left(\frac{h}{r_j}\right). \quad (7)$$

For interfering antennas, it can be noticed that since $r_j \gg h$, we have $\phi_j = \arctan\left(\frac{h}{r_j}\right) \rightarrow 0$, and $\left(\frac{\phi_j - \phi_{tilt}}{\phi_{3dB}}\right)^2 \rightarrow \left(\frac{\phi_{tilt}}{\phi_{3dB}}\right)^2$. Therefore the vertical antenna pattern (5) can be written as:

$$\begin{aligned} A_{v_{dB}}(\phi) &= -\min\left[12\left(\frac{\phi - \phi_{tilt}}{\phi_{3dB}}\right)^2, A_m\right] \\ &\approx -\min\left[12\left(\frac{\phi_{tilt}}{\phi_{3dB}}\right)^2, A_m\right] \\ &= G_{v_{dB}}, \end{aligned} \quad (8)$$

where $G_{v_{dB}} = -\min\left[12\left(\frac{\phi_{tilt}}{\phi_{3dB}}\right)^2, A_m\right]$ (i.e. a constant). And the antenna gain can be expressed as:

$$\begin{aligned} A_{dB}(\theta, \phi) &= -\min[-A_{h_{dB}}(\theta) - A_{v_{dB}}(\phi), A_m] \\ &= -\min[-A_{h_{dB}}(\theta) - G_{v_{dB}}, A_m] \\ &= -\min[-A_{h_{dB}}(\theta), A_m + G_{v_{dB}}] + G_{v_{dB}} \\ &= B_{dB}(\theta) + G_{v_{dB}}, \end{aligned} \quad (9)$$

where $B_{dB}(\theta) = -\min[-A_{h_{dB}}(\theta), A_m + G_{v_{dB}}]$.

So we have:

$$\begin{cases} B_{dB}(\theta) = -\min[-A_{h_{dB}}(\theta), A_m + G_{v_{dB}}] \\ G_{v_{dB}} = -\min\left[12\left(\frac{\phi_{tilt}}{\phi_{3dB}}\right)^2, A_m\right] \end{cases} \quad (10)$$

Therefore, we establish that in this case, the vertical antenna gain only depends on the angle θ .

C. 3D Analytical SINR Expression

Considering a density ρ_S of sites S and following the approach developed in [9] [10], let us consider a UE located at (R_i, θ_i, ϕ_i) in the area covered by the base station i .

Since each site is equipped by 3 antennas, we can express the denominator of (2) as:

$$I = G_0 \int 3 \times \rho_S K P R^{-\eta} A(\theta, \phi) t dt d\theta + PKR_i^{-\eta} \sum_{a=2}^3 A(\theta_i^a, \phi_i^a) + N_{th}, \quad (11)$$

where the integral represents the interference due to all the other sites of the network, and the discrete sum represents the interference due to the 2 antennas co-localized with the antenna i . The index a holds for these 2 antennas.

This can be further written as:

$$I = G_0 \int P \rho_S K (t^2 + h^2)^{-\frac{\eta}{2}} t dt \times 3 \int A(\theta, \phi) d\theta + PK(r_i^2 + h^2)^{-\frac{\eta}{2}} \sum_{a=2}^3 A(\theta_i^a, \phi_i^a) + N_{th}. \quad (12)$$

Since for the other sites of the network, the distance $r \gg h$, we have $(t^2 + h^2)^{-\frac{\eta}{2}} = t^{-\eta} (1 + h^2/t^2)^{-\frac{\eta}{2}} \approx t^{-\eta}$, and the interference can be approximated by using (9):

$$I = G_0 \int P \rho_S K t^{-\eta} t dt G_v \times 3 \int_0^{2\pi} B(\theta) d\theta + PK(r_i^2 + h^2)^{-\frac{\eta}{2}} \sum_{a=2}^3 A(\theta_i^a, \phi_i^a) + N_{th}, \quad (13)$$

where $G_v = 10^{\frac{G_{v,dB}}{10}}$. The approach developed in [9] [10] allows to express $\int P \rho_S K r^{-\eta} t dt$ as $\frac{\rho_S PK (2R_c - r_i)^{2-\eta}}{\eta-2}$, where $2R_c$ represents the intersite distance (ISD). We refer the reader to [9] [10] for the detailed explanation. Therefore, (13) can be expressed as:

$$I = G_0 \frac{3G_v PK (2R_c - r_i)^{2-\eta}}{\eta-2} \rho_S \int_0^{2\pi} B(\theta) d\theta + PK(r_i^2 + h^2)^{-\frac{\eta}{2}} \sum_{a=2}^3 A(\theta_i^a, \phi_i^a) + N_{th}. \quad (14)$$

For a UE located at (r, θ, ϕ) (dropping the index i) relatively to its serving base station, the inverse of the SINR (2) is finally given by the expression:

$$\frac{1}{\gamma(r, \theta, \phi)} = \frac{3G_v \rho_S (2R_c - r)^{2-\eta} \int_0^{2\pi} B(\theta) d\theta}{(\eta-2)(r^2 + h^2)^{-\eta/2} A(\theta, \phi)} + \frac{\sum_{a=2}^3 A(\theta_i^a, \phi_i^a)}{A(\theta, \phi)} + \frac{N_{th}}{G_0 PK (r^2 + h^2)^{-\eta/2} A(\theta, \phi)}, \quad (15)$$

where the index a holds for the 2 antennas co-localized with the serving antenna i . Let notice that since R is a function of r , we can express the SINR $\gamma(R, \theta, \phi)$ as $\gamma(r, \theta, \phi)$.

D. Interest of the Analytical Formula

The SINR expression (2) depends on the distances and the angles between the UE and all the base stations of the network. Therefore, simulations are needed to compute the expression of the SINR in the aim to evaluate the SINR values. It can

be moreover noticed that this formula is intractable for further evaluations.

In the opposite, the closed form formula (15) allows the calculation of the SINR in an easy way. First of all, it no longer depends on the distances of the UE to all the base stations, but only on the distance to its serving base station, the antenna gains of this serving base station and the co-localized base stations. Moreover, this formula allows to focus on the characteristic parameters of the network impacting the SINR (the topological parameter: inter-site distance, the propagation parameter: path-loss parameter and antenna gain). It also highlights the other sites impact, the co-localized base stations and the thermal noise impact on the SINR. Since that formula is tractable, a simple numerical calculation is needed.

E. Throughput Calculation

The SINR allows calculating the maximum theoretical achievable throughput D_u of a UE u , by using Shannon expression. For a subcarrier bandwidth W , it can be written:

$$D(u) = W \log_2(1 + \gamma(u)) \quad (16)$$

Remark: In the case of realistic wireless network systems, it can be noticed that the mapping between the SINR and the achievable throughput are established by the mean of *level curves*.

III. VALIDATION OF THE ANALYTICAL FORMULA

The validation of the analytical formula (15) consists in the comparison of the results established by this formula, to the ones established by Monte Carlo simulations.

A. Assumptions

Let us consider:

- A hexagonal network composed of sectored sites;
- Three base stations per site;
- The 2D model: the antenna gain of a transmitting base station is given in dB by:

$$G_T(\theta) = -\min \left[12 \left(\frac{\theta}{\theta_{3dB}} \right)^2, A_m \right], \quad (17)$$

where $\theta_{3dB} = 70^\circ$ and $A_m = 21$ dB;

- The 3D model: the antenna gain of a transmitting base station is given by expressions (3) (4) (5);
- Analyzed scenarios corresponding to realistic situations in a network:
 - Urban environment: Inter Site Distance ISD = 200m, 500m and 750m,
 - Antennas tilts: 20° , 30° , 40° .

B. Simulations vs 3D Analytical Model

User equipments are randomly distributed in a cell of a 2D hexagonal based network (Fig. 2). This hexagonal network is equipped by antennas which have a given height (30m and 50m in our analysis), in the third dimension. Monte Carlo simulations are done to calculate the SINR for each UE. We

focus our analysis on a typical hexagonal site. The cumulative distribution function (CDF) of the SINR can be established by using these simulations. These curves are compared to the ones established by using the analytical formula (15) to calculate the SINR values. Moreover, the SINR values established by the two ways are drawn on figures representing a site with three antennas.

We present two types of comparisons. We first establish the CDF of the SINR. Indeed, the CDF of SINR provides a lot of information about the network characteristics: the coverage and the outage probability, the performance distribution, and the quality of service that can be reached by the system. As an example, figure 3 shows that for an outage probability target of 10%, the SINR reaches -8 dB, which corresponds to a given throughput. A second comparison, focused on the values of the SINR at each location of the cell, establishes a map of SINR over the cell.

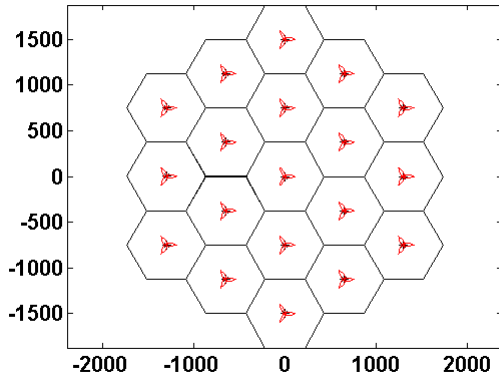


Figure 2. Hexagonal network: location of the 3 sectors base stations in the plan. The X and Y axes represent the coordinates, in meters. The intersite distance in this example is 750 m.

C. Results of the Validation

For the validation, we compare the two methods by considering realistic values of network parameters. An urban environment with realistic parameters of propagation is simulated [8]. Different tilts and apertures are considered. The scenarios, summarized in Tab. I, show that the 3D beamforming analytical model and the simulations provide very close values of SINR:

Table I
SCENARIOS AND FIGURES

Scenario	$\phi_{tilt}^{(\circ)}$	$\phi_{3dB}^{(\circ)}$	$\theta_{3dB}^{(\circ)}$	ISD (m)	h (m)	Figures
Scenario 1	30	10	10	500	50	3-4
Scenario 2	30	10	20	750	30	5-6-7
Scenario 3	20	10	10	750	30	8-9
Scenario 4	20	10	40	750	50	10-11
Scenario 5	40	30	20	750	30	12-13
Scenario 6	40	10	20	200	50	14-15

1) *CDF of SINR*: The figures of scenario 1 (Fig. 3), scenario 2 (Fig. 5 and 6), scenario 3 (Fig. 8), scenario 4 (Fig. 10), scenario 5 (Fig. 12) and scenario 6 (Fig. 14) show that the analytical model (blue curves) and the simulations (red curves) provide very close CDF of SINR curves.

2) *Map of SINR*: The figures of scenario 1 (Fig. 4), scenario 2 (Fig. 7), scenario 3 (Fig. 9), scenario 4 (Fig. 11), scenario 5 (Fig. 13) and scenario 6 (Fig. 15) represent the values of SINR in each location of a cell, where the X and Y axes represent the coordinates (in meters). These figures show that the analytical model (right side) and the simulations (left side) provide very close maps of SINR.

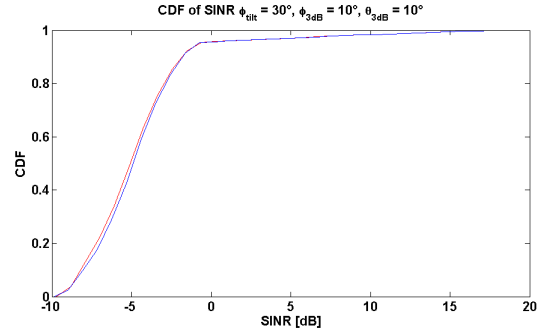


Figure 3. Comparison of CDF of SINR for $\phi_{tilt} = 30^\circ$, a vertical aperture $\phi_{3dB} = 10^\circ$ and an horizontal aperture $\theta_{3dB} = 10^\circ$.

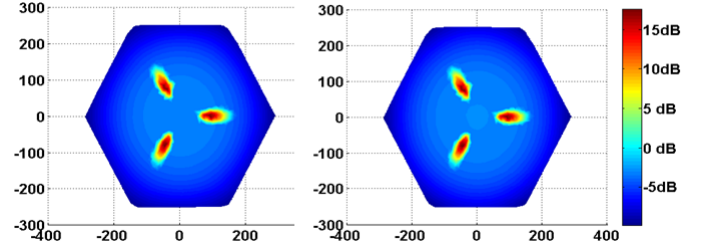


Figure 4. Simulation (left) and Analytical (right) Map of the SINR for $\phi_{tilt} = 30^\circ$, a vertical aperture $\phi_{3dB} = 10^\circ$ and an horizontal aperture $\theta_{3dB} = 10^\circ$.

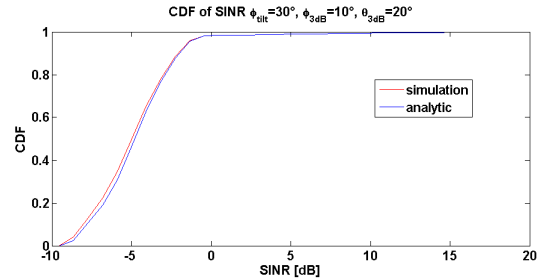


Figure 5. Comparison of CDF of SINR for $\phi_{tilt} = 30^\circ$, a vertical aperture $\phi_{3dB} = 10^\circ$ and an horizontal aperture $\theta_{3dB} = 20^\circ$.

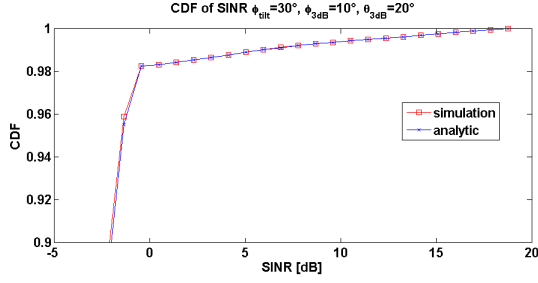


Figure 6. Zoom on the upper part of the CDF (Fig 5) where $\phi_{tilt} = 30^\circ$, $\phi_{3dB} = 10^\circ$ and $\theta_{3dB} = 20^\circ$.

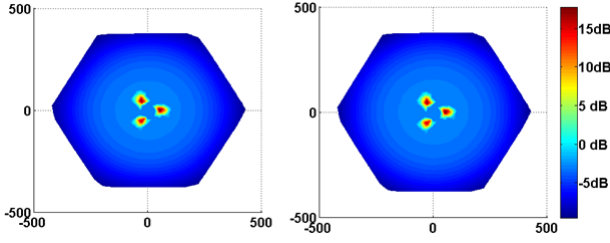


Figure 7. Simulation (left) and Analytical (right) Map of the SINR for $\phi_{tilt} = 30^\circ$, a vertical aperture $\phi_{3dB} = 10^\circ$ and an horizontal aperture $\theta_{3dB} = 20^\circ$.

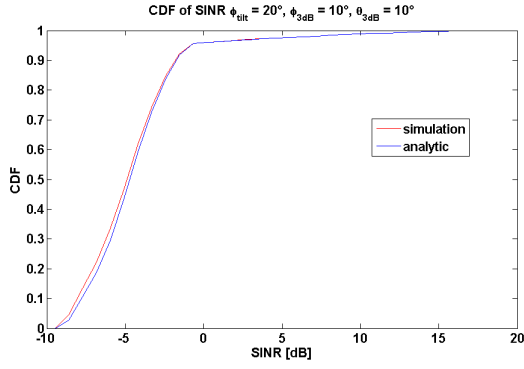


Figure 8. Comparison of CDF of SINR for $\phi_{tilt} = 20^\circ$, a vertical aperture $\phi_{3dB} = 10^\circ$ and an horizontal aperture $\theta_{3dB} = 10^\circ$.

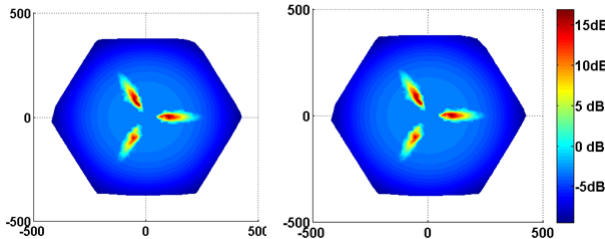


Figure 9. Simulation (left) and Analytical (right) Map of the SINR for $\phi_{tilt} = 20^\circ$, a vertical aperture $\phi_{3dB} = 10^\circ$ and an horizontal aperture $\theta_{3dB} = 10^\circ$.

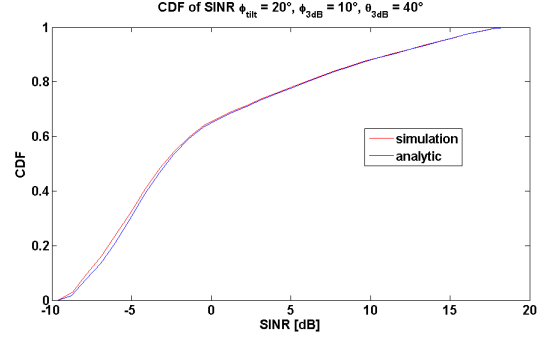


Figure 10. Comparison of CDF of SINR for $\phi_{tilt} = 20^\circ$, a vertical aperture $\phi_{3dB} = 10^\circ$ and an horizontal aperture $\theta_{3dB} = 40^\circ$.

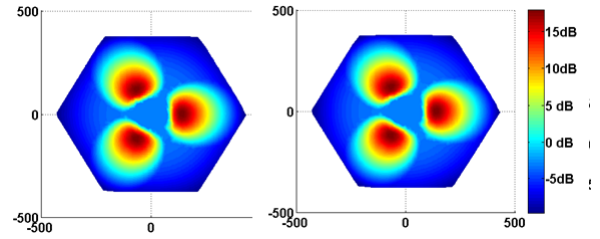


Figure 11. Simulation (left) Analytical (right) Map of the SINR for $\phi_{tilt} = 20^\circ$, a vertical aperture $\phi_{3dB} = 10^\circ$ and an horizontal aperture $\theta_{3dB} = 40^\circ$.

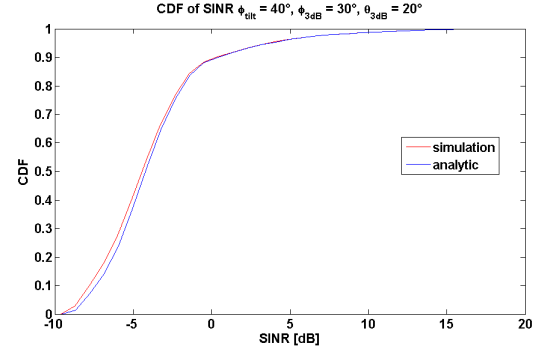


Figure 12. Comparison of CDF of SINR for $\phi_{tilt} = 40^\circ$, a vertical aperture $\phi_{3dB} = 30^\circ$ and an horizontal aperture $\theta_{3dB} = 20^\circ$.

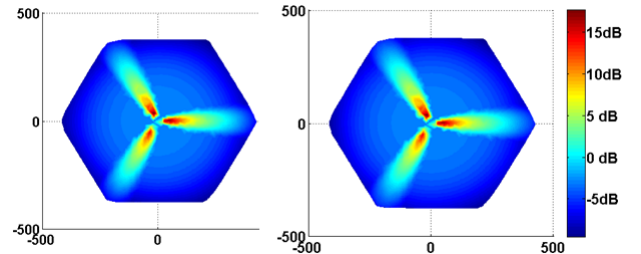


Figure 13. Simulation (left) and Analytical (right) Map of the SINR for $\phi_{tilt} = 40^\circ$, a vertical aperture $\phi_{3dB} = 30^\circ$ and an horizontal aperture $\theta_{3dB} = 20^\circ$.

D. Limitation of the 3D Beamforming Model

The aim of our analysis is to propose a model allowing to evaluate the performance reachable in a cell whose standard

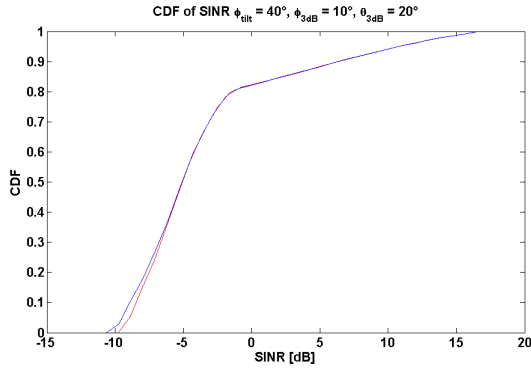


Figure 14. Comparison of CDF of SINR for $\phi_{tilt} = 40^\circ$, a vertical aperture $\phi_{3dB} = 10^\circ$ and an horizontal aperture $\theta_{3dB} = 20^\circ$.

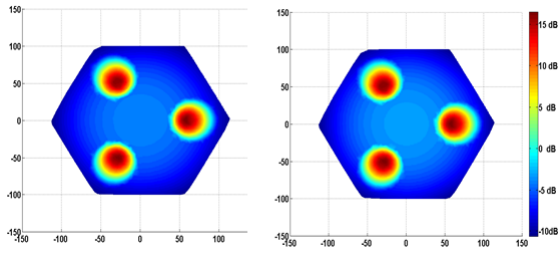


Figure 15. Simulation (left) and Analytic (right) Map of the SINR for $\phi_{tilt} = 40^\circ$, a vertical aperture $\phi_{3dB} = 10^\circ$ and an horizontal aperture $\theta_{3dB} = 20^\circ$.

antennas are replaced by beamforming antennas, and are focused on specific zones of the cell. This implies that the angle ϕ_{3dB} has to be lower than ϕ_{tilt} , otherwise UEs belonging to other cells could be served by this antenna. The validation process was done according to this constraint.

However, the analytical closed-form formula (15) allows to establish CDF of SINR very closed to simulated ones, for the different values of ϕ_{tilt} , vertical apertures ϕ_{3dB} and horizontal apertures θ_{tilt} , as soon as $\phi_{tilt} \geq \phi_{3dB}$. Moreover, the SINR maps given by simulations and by the formula are also very closed. Therefore, the formula is particularly well adapted for beamforming analysis.

IV. BEAMFORMING ANALYSIS WITH THE 3D MODEL

In this section, we show the interest of 3D beamforming and we compare its performance to 2D beamforming, a technique in which the tilt is not modified. We consider scenarios where the antennas are directed towards a specific zone, and have a low aperture in the two plans, horizontal and vertical. These scenarios allow focusing the energy in a small zone of the cell, and enable to mitigate the interferences. Moreover, the transmitted useful power is focused in a small zone, therefore the power received by a UE is higher due to the antenna gain. Using the 3D analytical beamforming model, the analysis may be done in a quick way.

A. 3D Beamforming Advantages

The curves (Fig. 3 to 15) show that the beamforming impact can be analyzed in a simple way. The CDF of SINR curves

Table II
COVERAGE FOR SINR ≥ 0 DB

Scenario	$\phi_{tilt}^{(\circ)}$	$\phi_{3dB}^{(\circ)}$	$\theta_{3dB}^{(\circ)}$	Coverage
Scenario 1	30	10	10	5%
Scenario 2	30	10	20	2%
Scenario 3	20	10	10	5%
Scenario 4	20	10	40	35%
Scenario 5	40	30	20	15%
Scenario 6	40	10	20	20%

show that values less than 0 dB may represent more than 98% of the curve (Fig. 5 and 6). This means that UEs located in more than 98% of the cell reach a SINR less than 0 dB, which is obvious in Fig. 7. The SINR values of the remaining UEs, distributed on 2% of the area, vary between 0 and 19 dB.

In fact, the objective of the beam is to focus the signal on a given small area, where the served UE is located. In this example, this area represents 2% of the cell. Table II gives the results for each scenario. The coverage of the beams, considering that the SINR has to reach a higher value than 0 dB, represents between 2 and 35% of the cell area, depending on the parameters values such as ϕ_{tilt} , ϕ_{3dB} and θ_{3dB} . This effect is also shown on the SINR maps, where best SINR areas are in red. This means that 3D beamforming allows to serve more precisely the users which need to receive data. A very small zone can be served as seen in the figures. The remaining area is not, or less, polluted by the electromagnetic emission. The beamforming allows also to focus the energy to areas far away from the serving base station. As observed in the map SINR figures, the zones covered by the beams may be far from antenna and still reach high level SINR. This is generally not the case in networks without beamforming.

Note that the extra gain obtained with 3D beamforming can be used to significantly reduce transmit power and thus save energy (with respect to a scenario without beamforming). Indeed, since the energy is concentrated in a small area, the antenna gain G_0 can reach a high level and therefore the transmitted power can be much lower than in a standard case. Typically for a beam with $\phi_{3dB} = 10^\circ$ and $\theta_{3dB} = 10^\circ$, the gain G_0 can reach about 26 dB. Therefore the transmitted power can be reduced by a factor 400. Moreover, the SINR received may reach the same value by reducing the transmitting power as expressed in (2).

B. 2D vs 3D Beamforming

The analysis consists in the comparison of the results established for 3D beamforming using the proposed 3D model to the ones established by simulations, where the 2D antenna gain is given by (17). Similarly to the validation case, we present two types of comparisons : the CDF of SINR (Fig. 16) and SINR maps over the cell, in the 2D and the 3D cases (Fig. 17).

The CDF curves drawn in Fig. 16 show that the 2D beamforming (blue curve) gives lower values of SINR than the 3D beamforming case (red curve). The difference can reach 6

dB (minimum SINR is -16 dB with 2D beamforming, and -10 dB with 3D beamforming). In terms of quality of service, this means that the outage probability is lower (i.e. better) in the 3D beamforming case than in the 2D one. This is true until a SINR value of -5dB (CDF value 0.35). This correspond to 35 % of UEs of the cell. For higher values of SINR the 2D case gives a better CDF than the 3D one. The two curves reach a maximum SINR value of 18 dB. We thus observe a wider range of SINR values with 2D beamforming. This means that the beam is much less focused with 2D than with 3D beamforming and this is of course due to the fact that with 3D beamforming it is possible to modify the tilt.

Moreover, it can be observed that the locations of highest SINR values are very different in the two cases. The SINR maps over the cell in the 2D and the 3D cases (Fig. 17) show that in the 3D beamforming case, UEs far from the BS reach higher SINR values than UEs close to the BS, even far from the serving base station (Fig. 17 left). This result is not possible in the 2D case (Fig. 17 right). In this case the best SINR values are located close to the base station. And the zone of high SINR is more distributed over the cell than in the 3D case.

Observe the SINR map of Fig. 17 right. The UEs located in the main direction of one of the three beams will experience a SINR ranging from 0 to 18 dB depending on their distance to the base station. This is because the base station is not able to adjust the tilt to the distance. On the contrary, the base station can focus directly a 3D beam with high accuracy to the UE location (see Fig. 17 left) so that the experienced SINR reaches 15 dB or more.

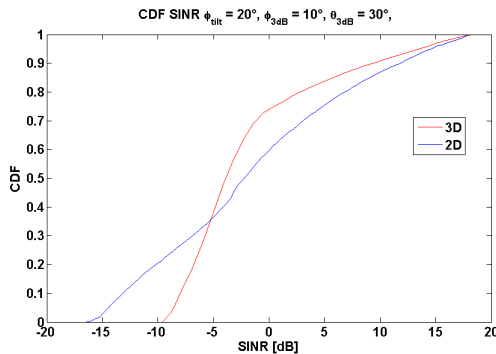


Figure 16. Comparison of the CDF of the SINR for urban environment (ISD=300m), using a 3D model and a 2D model of beamforming, $\phi_{tilt} = 20^\circ$, $\phi_{3dB} = 10^\circ$, $\theta_{3dB} = 30^\circ$

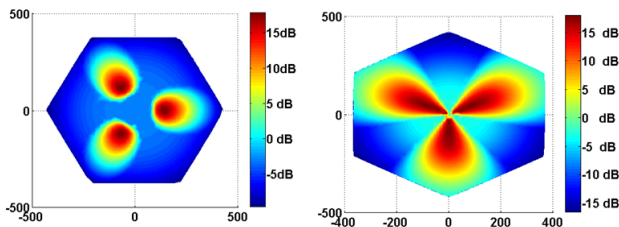


Figure 17. SINR Map 3D (left) and 2D (right) for $\phi_{tilt} = 20^\circ$, a vertical aperture $\phi_{3dB} = 10^\circ$ and an horizontal aperture $\theta_{3dB} = 30^\circ$.

V. CONCLUSION

We developed, and validated, a 3D beamforming analytical model of wireless networks. This model allowed us to establish a closed form formula of the SINR reached by a UE at any location of a cell. The validation of this model, by comparisons with the results given by Monte Carlo simulations showed that the two approaches establish very close results, in terms of CDF of SINR, and also in terms of SINR map of the cell. Moreover the analytical model allows a comparison between the 3D beamforming and the 2D beamforming. An analysis of the impact of 3D beamforming can be made, with a high accuracy and in a quick and easy way, by using this model. Further work includes the analysis of simultaneous multi-beam transmission and inter-beam interference.

REFERENCES

- [1] Valeria D'Amico, Carmen Botella, Jochen Giese, Richard Fritsche, Hardy Halbauer, Jörg Holfeld, Patrick Marsch, Stephan Saur, Tommy Svensson, Thorsten Wild, Wolfgang Zirwas. "Advanced Interference management in ARITST4G: Interference Avoidance". In *Wireless Technology Conference (EuWIT), 2010 European*, 2010.
- [2] M. Caretti, M. Crozzoli, G.M. Dell'Area, A.Orlando. "Cell Splitting Based on Active Antennas: Performance Assessment for LTE System". In *Wireless and Microwave Technology Conference (WAMICON), 2012 IEEE 13th Annual*, 2012.
- [3] Johannes Koppenborg, Hardy Halbauer, Stephan Saur, Cornelis Hoek. "3D Beamforming Trails with an Active Antenna Array". In *Smart Antennas (WSA), 2012 International ITG Workshop on*, 2012.
- [4] P. Chaipanya, P. Uthansakul, M. Uthansakul. "Reduction of Inter-Cell Interference Using Vertical Beamforming Scheme for Fractional Frequency Reuse Technique". In *Microwave Conference Proceedings (APMC), 2011 Asia-Pacific*, 2011.
- [5] Hardy Halbauer, Stephan Saur, Johannes Koppenborg, Cornelis Hoek. "Interference Avoidance with Dynamic Vertical Beamsteering in Real Deployment". In *Wireless Communications and Networking Conference Workshops (WCNCW)*, 2012.
- [6] Stephan Saur, Hardy Halbauer. "Exploring the Vertical Dimension of Dynamoc Steering". In *Multi-Carrier Systems & Solutions (MC-SS), 2011 8th International Workshop on*, 2011.
- [7] Osman N.C. Yilmaz, Seppo Hämäläinen, Jyri Hämäläinen. "System Level Analysis of Vertical Sectorization for 3GPP LTE". In *Wireless Communication Systems, 2009. ISWCS 2009. 6th International Symposium on*, 2009.
- [8] ITU-R. Guidelines for evaluation of radio interface technologies for imt-advanced, 12 2009.
- [9] Jean-Marc Kelif, Marceau Coupechoux and Philippe Godlewsk. "Spatial Outage Probability for Cellular Networks". In *Proc. of GLOBECOM*, 2007.
- [10] Jean-Marc Kelif, Marceau Coupechoux and Philippe Godlewsk. "On the Dimensioning of Cellular OFDMA Networks". In *PHYCOM118, online October 2011, DOI : 10.1016/j.phycom.2011.09.008*, 2009.
- [11] Jean-Marc Kelif, Marceau Coupechoux. "Cell Breathing, Sectorization and Densification in Cellular Networks". In *Modeling and Optimization in Mobile, Ad Hoc, and Wireless Networks, 2009. WiOPT 2009. 7th International Symposium on*, 2009.